Development of nitrification and elemental sulfur-based denitrification/anammox (NS^0DA) process for mainstream nitrogen removal

Liu, Yuanjun; Deng, Yangfan; van Loosdrecht, Mark C.M.; Chen, Guanghao

DOI
10.1016/j.watres.2025.123836

Publication date
2025

Document Version
Final published version

Published in
Water Research

Water Research 283 (2025) 123836

Contents lists available at ScienceDirect

Water Research

journal homepage: www.elsevier.com/locate/watres

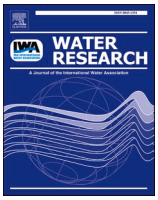

Development of nitrification and elemental sulfur-based denitrification/anammox (NS^0DA) process for mainstream nitrogen removal

Yuanjun Liu [a,b], Yangfan Deng [a,b,*], Mark C.M. van Loosdrecht [c], Guanghao Chen [a,b]

[a] Department of Civil and Environmental Engineering, Chinese National Engineering Research Center for Control & Treatment of Heavy Metal Pollution (Hong Kong Branch) and Water Technology Center, The Hong Kong University of Science and Technology, Hong Kong, China
[b] The Hong Kong University of Science and Technology, Shenzhen Research Institute, Shenzhen 518000, China
[c] Department of Biotechnology, Delft University of Technology, Delft, the Netherlands

ARTICLE INFO

Keywords:
Mainstream wastewater treatment
Biological nitrogen removal
Anammox
Sulfur-based denitrification

ABSTRACT

The implementation of mainstream anaerobic ammonium oxidation (anammox) can facilitate the realization of carbon-neutral wastewater treatment. However, this technology remains challenging owing to the inability to stably provide nitrite. In this study, we developed a novel nitrification and elemental sulfur-based partial autotrophic denitrification/anammox (NS^0DA) process for mainstream nitrogen removal. The NS^0DA system consists of a nitrification reactor and a combined elemental sulfur-based denitrification and anammox (S^0DA) reactor. Each reactor was independently initiated and optimized before being integrated. At mainstream nitrogen levels (48.5 ± 1.7 mg NH_4^+-N/L) and 25 °C, the NS^0DA system achieved 89.1 ± 5.7 % total nitrogen (TN) removal efficiency, with an effluent TN concentration of 5.4 ± 2.8 mg N/L. The system exhibited a low N_2O emission factor (0.23 %), significantly lower than other anammox-based systems. The S^0DA reactor achieved a nitrogen removal rate of 0.53 kg N/(m^3·d) with a short hydraulic retention time (2 h). Anammox accounted for 87.3 ± 7.0 % of the TN removal in the S^0DA reactor. Isotope experiments and kinetic analysis revealed the cooperation between anammox and denitrification for nitrogen removal. Polysulfides formed in the S^0DA reactor enhanced the utilization rate of elemental sulfur. High-throughput sequencing identified *Thiobacillus* and *Candidatus* Brocadia as the dominant genera of sulfur oxidation and anammox, respectively. The nitrogen and sulfur metabolic pathways were further verified through metagenomic analysis. Overall, the NS^0DA process provides a stable and efficient nitrogen removal process, minimizing oxygen demand, eliminating organic carbon requirements, and reducing N_2O emissions compared to conventional nitrification/denitrification. This approach offers a promising solution for mainstream nitrogen removal in wastewater treatment.

1. Introduction

Wastewater treatment plants (WWTPs) are pivotal in addressing water-energy-sanitation challenges. However, conventional activated sludge processes are energy-intensive (Li et al., 2015; McCarty et al., 2011). Anaerobic ammonium oxidation (anammox) is an autotrophic nitrogen removal process that does not consume organic carbon, enabling the decoupling of carbon and nitrogen removal in wastewater treatment (McCarty, 2018). Combining energy recovery from carbon capture with anammox-driven nitrogen removal for sewage treatment can make WWTPs energy-neutral or even energy-positive (Kartal et al., 2010).

Despite extensive research on anammox, implementing mainstream anammox remains a considerable challenge (Cao et al., 2017). This process typically relies on partial nitrification or partial denitrification to supply the required nitrite. While extensive studies have been conducted on partial nitrification-anammox (PNA), its mainstream application is hindered by unstable nitrite supply, despite strict control of operational parameters such as dissolved oxygen (DO), temperature, sludge retention time (SRT), and the use of various nitrite-oxidizing bacteria (NOB) inhibitors (Niederdorfer et al., 2021; Wang et al., 2023a). Compared with PNA, partial denitrification-anammox (PDA) demonstrates a consistent capacity to provide nitrite for anammox without complex control strategies to suppress NOB, and organic matter can be used as carbon sources (Du et al., 2019). However, excessive proliferation of heterotrophic denitrifiers in this combined system can

* Corresponding author.
E-mail address: ydengal@connect.ust.hk (Y. Deng).

https://doi.org/10.1016/j.watres.2025.123836
Received 28 February 2025; Received in revised form 22 April 2025; Accepted 14 May 2025
Available online 14 May 2025

outcompete anammox bacteria (AnAOB), deteriorating nitrogen removal performance (Kumar and Lin, 2010).

Reduced sulfur compounds (such as S^{2-}, S^0, and $S_2O_3^{2-}$) represent promising alternatives as electron donors for denitrification (Deng et al., 2022; Mulder, 1992). Among these reduced sulfur compounds, elemental sulfur offers distinct advantages, such as low price, non-toxicity, and easy availability (Sierra-Alvarez et al., 2007). Nitrite accumulation is commonly observed in elemental sulfur-based denitrification systems (Sierra-Alvarez et al., 2007; Yuan et al., 2022). Additionally, sulfur-oxidizing bacteria (SOB) and AnAOB exhibit comparable biomass yields and growth rates (Beffa et al., 1991; Zhang and Okabe, 2020), rendering it feasible to maintain balanced microbial communities in coculture systems. Thus, elemental sulfur-based denitrification combined with anammox (S^0DA) has attracted significant attention for sustainable nitrogen removal (Deng et al., 2022; Li et al., 2022). Although S^0DA has been applied for high-strength nitrate- and ammonium-containing wastewater in warm conditions (≥ 30 °C) (Li et al., 2019; Zhang et al., 2020), its potential for mainstream nitrogen removal remains to be explored.

This paper introduces a novel nitrification combined with S^0DA process (NS^0DA) for treating low-strength ammonium wastewater (i.e., 20–75 mg N/L). NS^0DA is a low-cost and fully autotrophic nitrogen removal process that can facilitate the establishment of energy-self-sufficient WWTPs with carbon capture and cost-effective nitrogen removal capabilities. However, several challenges remain in the implementation of NS^0DA. First, the stable and efficient supply of nitrite for anammox by elemental sulfur-based denitrification is a challenge. It was reported that well-controlled conditions, such as high temperature (≥ 30 °C) and high pH (≥ 8.5), are essential for elemental sulfur-based partial denitrification (Chen et al., 2018; Li et al., 2023). Second, the nitrogen removal efficiency of the NS^0DA process remains to be investigated. The application potential of NS^0DA is contingent on achieving a satisfactory nitrogen removal rate (NRR), which is hindered by the low bioavailability of elemental sulfur (Boulegue, 1978; Di Capua et al., 2016). The capability of NS^0DA to overcome this technical barrier remains to be clarified.

Therefore, this study aimed to (1) investigate the feasibility of the NS^0DA process for treating mainstream wastewater at 25 °C, (2) analyze N-removal pathways within the NS^0DA system, (3) reveal the utilization mechanisms of elemental sulfur, and (4) clarify the microbial community dynamics during the operation of the NS^0DA process.

2. Materials and methods

2.1. Operational strategies for continuous reactors

The NS^0DA system was composed of a nitrification reactor and an S^0DA reactor. The NS^0DA process is schematically illustrated in Fig. 1. The operation of NS^0DA process was divided into phases I and II. Phase I involved the independent startup and optimization of the nitrification and S^0DA reactors. In Phase II, the two reactors were integrated to establish the NS^0DA process.

2.1.1. Phase I: separate operation of nitrification and S^0DA reactors

A moving bed biofilm reactor (MBBR) with a working volume of 0.5 L was used for nitrification. This reactor used the Mutag BioChip 30™ carrier (protected active surface area of 5500 m^2/m^3) with a filling ratio of 20 %. Biofilm-covered carriers were sourced from a 2 L biofilm reactor in the laboratory. The MBBR operated in the continuous flow mode with a hydraulic retention time (HRT) of 4 h at 25 °C. The DO concentration in the reactor was maintained above 5.0 mg/L. The MBBR was fed with synthetic wastewater containing 50 mg N/L NH_4^+ and mineral media (Table S1).

The S^0DA process was implemented in an up-flow anaerobic sludge blanket (UASB) reactor with a working volume of 0.5 L, diameter of 6.5 cm, and height of 15 cm. A three-phase separator was installed at the top of the reactor. The seeding sludge for the S^0DA reactor was sourced from a combined sulfide-based partial denitrification and anammox system (Deng et al., 2021). The concentrations of initial suspended solids (SS) and volatile suspended solids (VSS) in the reactor were 7.02 and 5.74 g/L, respectively. To enhance mixing intensity, a peristaltic pump continuously circulated the produced gas from the reactor headspace to its bottom, with a recycling ratio of the gas flowrate to the influent flowrate of 1.3. Phase I operations of the S^0DA system were divided into three phases (Table 1). In Phase IA, S^0DA was rapidly initiated at 30 °C, with influent NO_3^- and NH_4^+ concentrations each set at 50 mg N/L. In Phases IB and IC, the performance of S^0DA was evaluated using low-strength wastewater (NH_4^+/NO_3^- = 25/25 mg N/L) at 30 °C and 25

Table 1
Operating conditions of the S^0DA system in Phase I.

Phase	Time d	HRT h	NO_3^- mg N/L	NH_4^+ mg N/L	NLR kg N/(m^3·d)	Temperature °C
IA	1–54	5	50	50	0.48	30
IB	55–109	2	25	25	0.60	30
IC	110–143	2	25	25	0.60	25

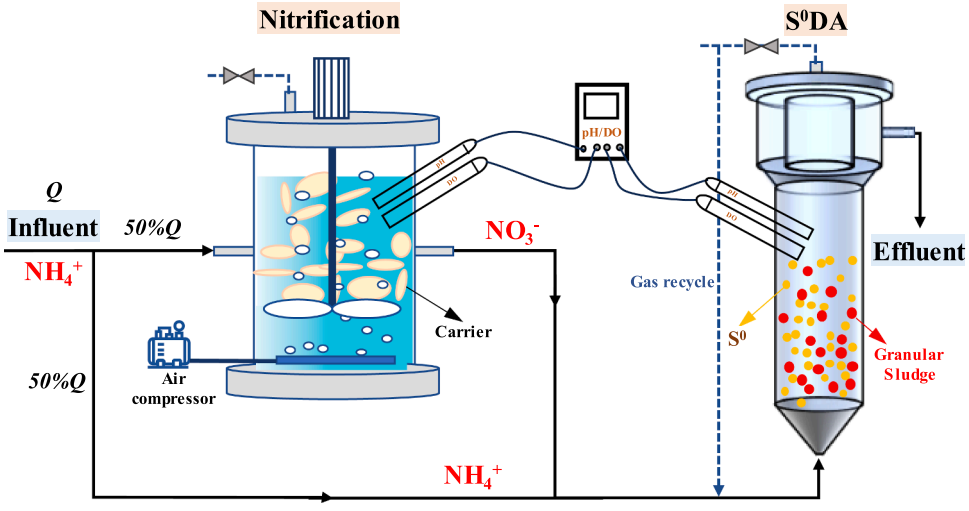

Fig. 1. Schematic of the NS^0DA process.

°C, respectively. The detailed composition of synthetic wastewater is presented in Table S1. Elemental sulfur powder was added daily according to the nitrogen loading rate (NLR).

2.1.2. Phase II: operation of the NS^{0}DA system

After 143 days of independent operation, the nitrification and S^{0}DA reactors were integrated to establish the NS^{0}DA system (Fig. 1). The influent stream contained 50 mg N/L NH_4^+ and mineral media (Table S1). Synthetic wastewater was fed to the MBBR and S^{0}DA reactor in series, with a bypass flow of 50 %. The HRTs for the nitrification and S^{0}DA reactors were 4 and 2 h, respectively. The NLRs for the nitrification and S^{0}DA reactors were 0.30 and 0.60 kg N/(m^3·d), respectively. The NS^{0}DA system operated at 25 °C throughout Phase II.

2.2. Batch experiments for S^{0}DA

2.2.1. ^{15}N isotope labeling experiment

At the end of Phase II, nitrogen removal pathways in the S^{0}DA reactor were evaluated through a ^{15}N isotope labeling experiment. Biomass (295 ± 13 mg VSS) obtained from the S^{0}DA reactor was washed three times with deionized water and transferred into a 120 mL serum bottle with a working volume of 100 mL. The biomass was resuspended in 100 mL of mineral medium (Table S1). Subsequently, the bottle was thoroughly purged with helium gas (99.999 %) to eliminate nitrogen and oxygen from the reactor. The serum bottle was allowed to stabilize for 1 h under the action of a magnetic stirrer (200 rpm) at 25 °C, and the batch test was initiated by adding 2.5 mg $^{14}NH_4^+$-N and 2.5 mg $^{15}NO_3^-$-N. $^{29}N_2$ and $^{30}N_2$ in the headspace of the serum bottle were collected and measured using isotope ratio mass spectrometry (MAT253, Gas Bench, USA) throughout the batch test. Simultaneously, the concentrations of NH_4^+, NO_2^-, NO_3^-, N_2O, and SO_4^{2-} in the liquid phase were monitored. This batch test was conducted in triplicate.

2.2.2. Determination of polysulfide anions in the S^{0}DA reactor

To determine the role of polysulfides in sulfur metabolism in the S^{0}DA reactor, a batch test was conducted under anaerobic conditions without nitrate. After three rounds of washing with deionized water, the sludge was evenly distributed into three parallel serum bottles and resuspended in 100 mL of mineral medium (Table S1) without NO_3^- and NH_4^+. The biomass concentration in these bottles was 2.0 g VSS/L. Each bottle was supplemented with 100 mg of elemental sulfur powder. After deoxygenation, the batch experiment was conducted by placing the bottles on a magnetic stirrer (200 rpm) at 25 °C for 20 h. Sulfide, sulfate, and polysulfides concentrations in the reactor were measured during the experiment.

2.3. Physical and chemical analysis

NH_4^+, SS, and VSS were detected following standard methods (Rice et al., 2005). The concentrations of NO_3^-, NO_2^-, and SO_4^{2-} were determined using an ion chromatography device (Thermo Fisher Scientific, USA) equipped with a Dionex IonPac AS19 column. Gas- and liquid-phase concentrations of N_2O were measured using a gas chromatography device equipped with a thermal conductivity detector (Agilent Technologies 7890A GC, USA) and an N_2O microsensor (N_2O-R, Unisense, Denmark), respectively. The pH and DO values were monitored using MultiLine® IDS portable meters (WTW 3620, German). Polysulfide samples were stabilized using methyl triflate (C_3FSO_3Me) to form stable dimethyl polysulfides (Me_2S_x) (Kamyshny et al., 2004). After derivatization, the samples were immediately analyzed using a high-performance liquid chromatography (HPLC, Agilent 1260 Infinity II, USA) equipped with a C18 column (COSMOSIL 5C18-PAQ, 4.6 mm I. D. × 250 mm).

2.4. Calculations

2.4.1. Nitrogen removal pathways in the S^{0}DA reactor

Nitrogen removal pathways in the S^{0}DA reactor were evaluated through calculations and experiments. Based on the long-term performance of the S^{0}DA reactor, the contributions of anammox (C_{an}) and denitrification (C_{dn}) to nitrogen removal were determined using Eqs. (1) and (2), respectively.

$$C_{an} = 1.974 \times \frac{\Delta NH_4^+ - N}{\Delta TN} \times 100\% \quad (1)$$

$$C_{dn} = 100\% - C_{an} \quad (2)$$

where ΔNH_4^+-N and ΔTN represent the amounts of NH_4^+ and total nitrogen (TN) removed in the S^{0}DA reactor, respectively. The factor 1.974 represents the mass concentration ratio between nitrogen gas produced and NH_4^+ removed in the anammox process (Lotti et al., 2014).

Moreover, the nitrogen removal pathways in the S^{0}DA reactor were directly estimated by measuring the yields of $^{29}N_2$ and $^{30}N_2$, using $^{14}NH_4Cl$ and $Na^{15}NO_3$ (≥ 98 atom % ^{15}N) as substrates in the batch tests. Assuming that nitrogen gas produced by anammox contains one nitrogen atom each from NH_4^+ and NO_3^-, $^{28}N_2$ and $^{29}N_2$ gases are formed. Sulfur-based denitrification can also generate $^{28}N_2$, $^{29}N_2$ and $^{30}N_2$. The corresponding conversion relationships are as follows (Thamdrup and Dalsgaard, 2002):

$$A_{total} = \frac{A_{28}}{1-p} = \frac{A_{29}}{p} \quad (3)$$

$$D_{total} = \frac{D_{28}}{(1-p)^2} = \frac{D_{29}}{2 \times (1-p) \times p} = \frac{D_{30}}{p^2} \quad (4)$$

where $A_{28}/A_{29}/A_{total}$ and $D_{28}/D_{29}/D_{30}/D_{total}$ represent the N_2 produced through anammox and denitrification, respectively. p represents the proportion of ^{15}N in NO_3^-. Based on the yields of $^{29}N_2$ (Y_{29}) and $^{30}N_2$ (Y_{30}, Y_{30}=D_{30}), A_{total} and D_{total} can be calculated using Eqs. (5) and (6), respectively.

$$A_{total} = \frac{Y_{29} - Y_{30} \times 2 \times (p^{-1} - 1)}{p} \quad (5)$$

$$D_{total} = \frac{Y_{30}}{p^2} \quad (6)$$

2.4.2. N_2O emission factor of the NS^{0}DA system

The N_2O emission factor (r_{N_2O-N}) of the NS^{0}DA system was estimated using the following equation:

$$r_{N_2O-N} = \frac{Q_{gas} \times C_{gas} \times 10^{-6} \times m_V \times M_N}{Q_{Inf.} \times TN} \quad (7)$$

where Q_{gas} is the volume of gas emitted from the reactor (L/d), C_{gas} is the N_2O concentration in the emitted gas (ppmv), m_V is the molar volume of N_2O at standard conditions (0.041 mol/L), M_N is the molar mass of N in N_2O (28 g/mol), $Q_{Inf.}$ is the influent flow rate of the reactor (L/d), and TN is the TN concentration in the influent (g N/L).

2.5. Microbial analysis

Sludge samples were collected from the S^{0}DA reactor on days 50 (Phase IA), 100 (Phase IB), 140 (Phase IC), 240 (Phase II), and 340 (Phase II). Additionally, two biomass samples were collected from the carriers in the MBBR on days 140 and 340. DNA was extracted from these samples using the magnetic soil and stool DNA kit (Tiangen, Beijing, China). Polymerase chain reaction (PCR) amplification targeted the V3-V4 region of the extracted DNA fragments. Subsequently, the purified PCR products were subjected to library construction and sequenced

on the Illumina NovaSeq6000 platform (Novogene Co., Ltd.).

Samples collected from the S^0DA reactor on days 50, 100, 140, and 340 were subjected to metagenomic sequencing on the Illumina sequencing platform (Novogene Co., Ltd.). After quality control, the clean data were assembled using MEGAHIT software. Open reading frames (ORFs) were predicted for the scaftigs using MetaGeneMark, and a non-redundant gene catalogue was constructed by removing redundancy (Nielsen et al., 2014). Functional annotations were performed by comparing the gene catalogue against the Kyoto Encyclopedia of Genes and Genomes (KEGG) database using DIAMOND software (Kanehisa et al., 2017).

3. Results and discussion

3.1. Phase I: separate operation of nitrification and S^0DA reactors

In Phase I, the nitrification and S^0DA reactors were operated separately. Nitrification was performed in the MBBR, and the S^0DA process was initiated in the UASB. The operating conditions of each reactor were optimized to achieve stable performance and prepare for the establishment of the NS^{0}DA process.

3.1.1. Achieving nitrification in the MBBR

In Phase I, the MBBR achieved complete nitrification at 25 °C, as shown in Fig. 2. The influent contained 47.4 ± 2.2 mg N/L ammonium and 1.6 ± 1.3 mg N/L nitrite. Robust nitrification performance was observed throughout this period, with an average NH_4^+ removal efficiency of 98.9 ± 1.3 %, and the effluent NH_4^+ concentration was consistently low at 0.5 ± 0.6 mg N/L. The effluent concentrations of NO_3^- and NO_2^- were 47.8 ± 2.3 and 0.5 ± 0.7 mg N/L, respectively. Nitrate was the main nitrogen species in the effluent, accounting for 97.8 ± 2.4 % of the effluent TN. Nitrogen loss owing to denitrification and anammox was negligible, given the absence of organics and high DO concentration in the nitrifying MBBR. The nitrification kinetics in the reactor were investigated. In the in-situ batch test, 45.5 mg N/L NH_4^+ was eliminated within 2.75 h, less than the HRT of the MBBR (4 h) (Fig. S1). These results indicated that the reactor has a higher potential for nitrifying activity. Overall, the MBBR demonstrated effective and reliable nitrification performance, establishing the necessary conditions for the NS^{0}DA process.

3.1.2. Realizing robust and high-rate nitrogen removal in the S^0DA reactor

The nitrogen removal performance of the S^0DA reactor was evaluated over 140 days of operation, divided into three phases based on different NLRs and temperatures. Phase IA represented the quick startup period, in which the S^0DA reactor was operated at 30 °C with influent ammonium and nitrate concentrations of 47.7 ± 1.5 and 49.4 ± 1.8 mg N/L (Figs. 3a & b), respectively. The NLR in Phase IA was maintained at 0.47 ± 0.01 kg N/(m^3·d). As shown in Fig. 3c, the S^0DA reactor rapidly started up within 13 d, achieving a TN removal efficiency of 93.2 %. Subsequently, stable nitrogen removal was gradually achieved, with a TN removal efficiency of 98.6 ± 1.3 % at the end of Phase IA (38–54 d, n = 15). The effluent concentrations of NH_4^+ and NO_3^- were 0.9 ± 0.8 and 0.2 ± 0.7 mg N/L, respectively. In the assessment of the feasibility of the S^0DA reactor for treating mainstream wastewater, the influent NH_4^+ and NO_3^- concentrations were decreased to 23.6 ± 0.9 and 25.5 ± 0.7 mg N/L, respectively, in Phase IB. Additionally, the HRT was shortened to 2 h, with an NLR of 0.60 ± 0.01 kg N/(m^3·d). In Phase IB (94–109 d, n = 16), the TN removal efficiency remained 97.6 ± 2.4 %, and the NRR increased from 0.46 ± 0.02 kg N/(m^3·d) (Phase IA) to 0.59 ± 0.02 kg N/(m^3·d). In Phase IC (110–143 d, n = 34), the operating temperature decreased to 25 °C. The effluent NH_4^+ and NO_3^- concentrations slightly increased to 5.6 ± 2.1 and 2.1 ± 1.4 mg N/L, respectively, and the TN nitrogen removal efficiency was 84.2 ± 3.1 %. The S^0DA reactor achieved a high NRR of 0.50 ± 0.02 kg N/(m^3·d) at 25 °C with an HRT of 2 h. The NRR of the S^0DA system was considerably higher than that of reported mainstream anammox systems, which typically achieved NRRs below 0.20 kg N/(m^3·d) (Hausherr et al., 2022; Lotti et al., 2015). These results highlight that elemental sulfur is an effective electron donor for the PDA process, supporting high-rate nitrogen removal.

The variation in sulfate concentration during long-term operation of the S^0DA reactor is shown in Fig. 3d Sulfate was the primary product of elemental sulfur oxidation, and other sulfur compounds (e.g., thiosulfate) were not detected in the reactor. In Phase IA, the average sulfate production was 72.0 mg S/L. Subsequently, as the influent nitrogen concentration was halved in Phase IB, the sulfate production decreased to 39.0 mg S/L. During Phase IC, the sulfate production slightly increased to 44.9 mg S/L. The variation in sulfate production was closely related to nitrate removal, and the mass ratio of sulfate production to nitrate removal (ΔSO_4^{2-}-S/ΔNO_3^--N) provided insights into the interactions between SOB and anammox bacteria in the S^0DA reactor. This ratio is 0.95 in the ideal S^0DA process, where the nitrite produced by SOB is completely consumed by anammox bacteria (Table S2). In contrast, this ratio is 2.51 for complete denitrification (Koenig and Liu, 2004; Strous et al., 1998). As shown in Fig. 3e, the ΔSO_4^{2-}-S/ΔNO_3^--N values were 1.2, 1.3, and 1.6 in Phases IA, IB, and IC, respectively. These findings suggested that SOB consumed more elemental sulfur in Phase IC than Phase IB, and the competitive ability of SOB against anammox

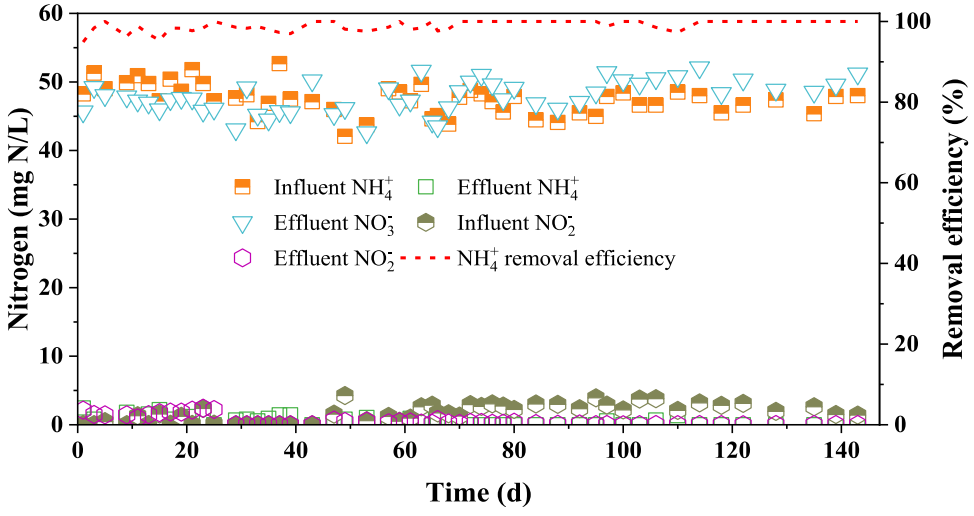

Fig. 2. Performance of the nitrification reactor in Phase I.

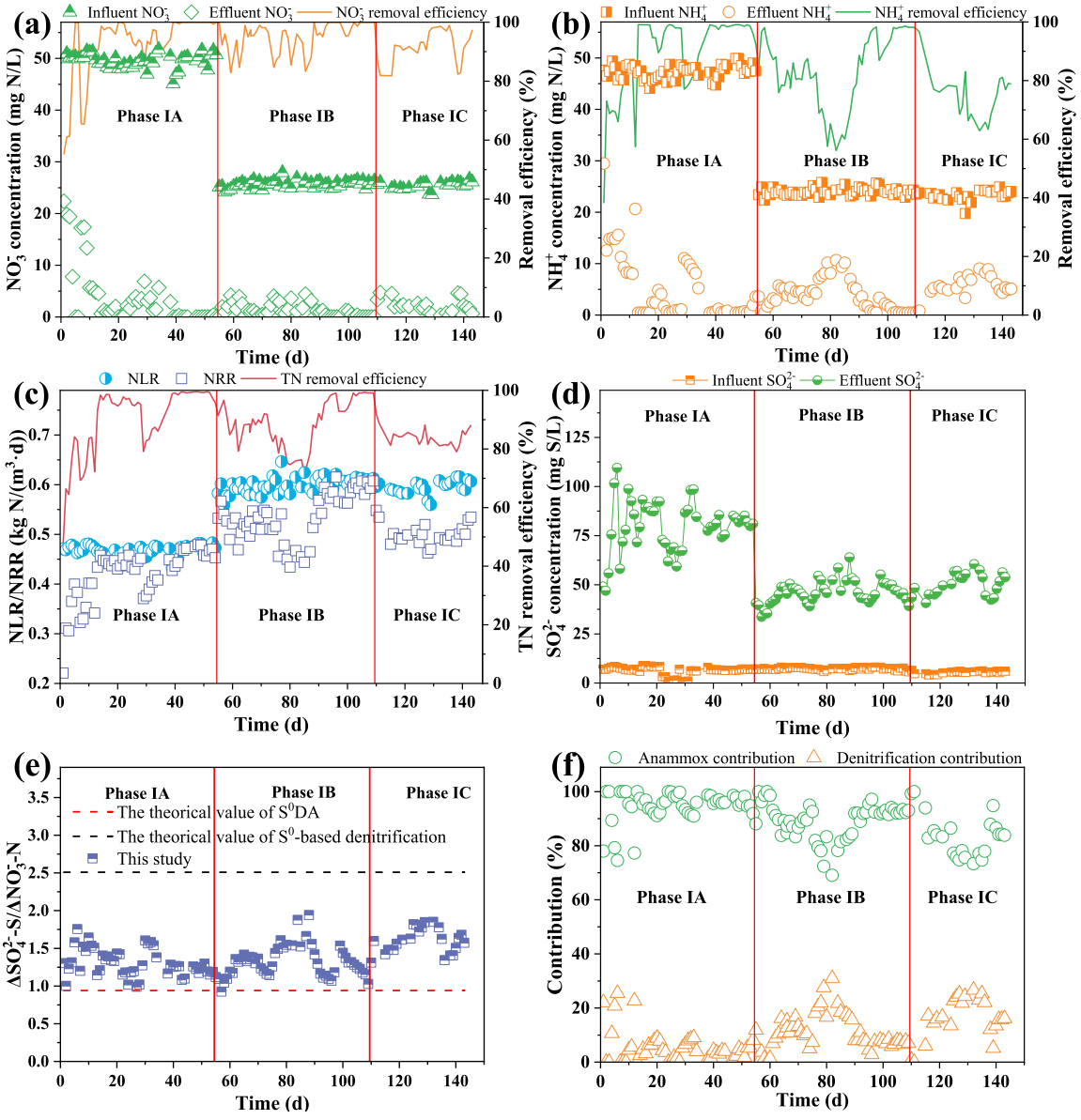

Fig. 3. Long-term performance of S^0DA reactor: variations in NO_3^- (a), NH_4^+ (b), TN, (c) and SO_4^{2-} (d) concentrations; mass ratio of SO_4^{2-} yield to NO_3^- removal (ΔSO_4^{2-}-S/ΔNO_3^--N) (e); and contribution of anammox and denitrification to nitrogen removal (f).

bacteria for nitrite increased at lower temperatures.

Anammox and elemental sulfur-based denitrification were the main pathways for nitrogen removal in the S^0DA reactor. Their respective contributions to nitrogen removal are shown in Fig. 3f. At the end of Phase IA, anammox contributed to 96.3 ± 1.8 % of nitrogen removal. This contribution slightly decreased to 93.1 ± 6.5 % in Phase IB, indicating that high anammox activity could be retained even at an HRT of 2 h and with low influent nitrogen. When the temperature was decreased to 25 °C in Phase IC, AnAOB exhibited higher sensitivity to the temperature change than SOB (Fig. S2). Nevertheless, anammox still contributed to 83.6 ± 7.6 % of nitrogen removal. In contrast, the contribution of anammox to nitrogen removal is typically below 80 % in organics-based mainstream PDA systems (Le et al., 2019; Takekawa et al., 2014). These results indicated that nitrite produced by SOB was mainly utilized by AnAOB, and further nitrite reduction by SOB was restricted in the S^0DA reactor. Suppressing nitrite reduction by SOB is crucial for realizing the S^0DA process. The factors contributing to the successful operation of the S^0DA can be summarised as follows. First, the residual nitrate (2.1 ± 1.4 mg N/L) in the S^0DA reactor prevented nitrite reduction by SOB. Nitrate reductase has a competitive advantage for electrons over nitrite reductase, especially in the presence of nitrate (Almeida et al., 1995; Glass and Silverstein, 1998). Second, AnAOB, as nitrite scavengers, limit the accessibility of nitrite for SOB. AnAOB exhibit a higher affinity for nitrite with a lower half-saturation constant for nitrite (Ks: 0.2–40.0 μM) compared with SOB (7.1–57.1 μM) (Wang et al., 2016; Zhang and Okabe, 2020).

3.2. Phase II: establishment and long-term operation of the NS^0DA process

After the startup and optimization of nitrification and S^0DA in separate reactors, these processes were integrated to establish the NS^0DA system. The NS^0DA was operated for 198 days in Phase II (from day 145 to day 342) to investigate its stability under mainstream conditions, and N_2O emissions from the combined process were evaluated.

3.2.1. Long-term performance of the NS^0DA process

The performance of the NS^0DA process is shown in Fig. 4. The

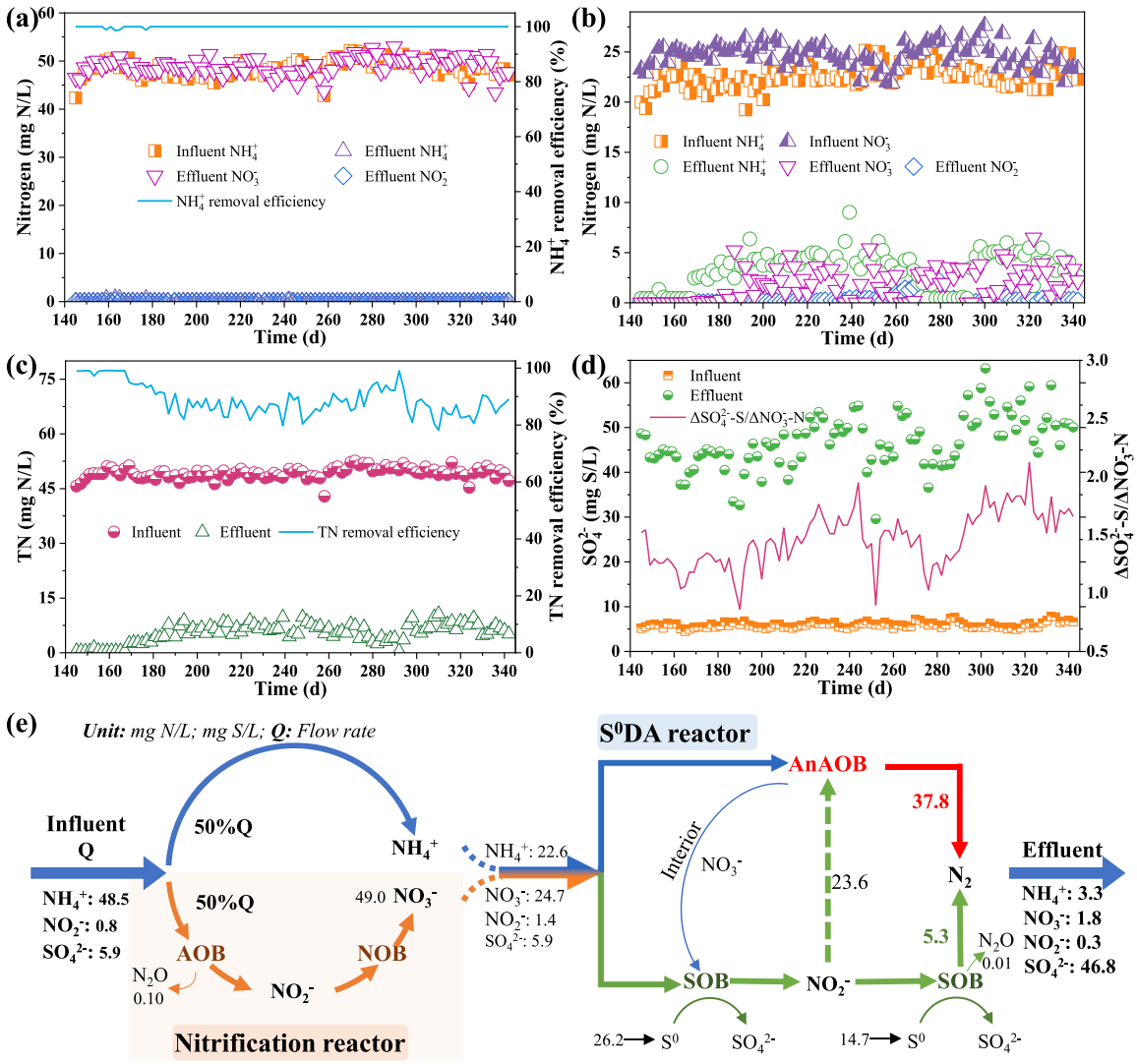

Fig. 4. Long-term performance of the NS^{0}DA process in Phase II: nitrification reactor (a); S^{0}DA reactor (b); TN concentration and TN removal efficiency of NS^{0}DA (c); SO_4^{2-} concentration and ΔSO_4^{2-}-S/ΔNO_3^--N in the S^{0}DA reactor (d); and nitrogen flux in the NS^{0}DA system (e).

influent ammonium concentration was maintained at 48.5 ± 1.7 mg N/L in Phase II. Half of the ammonium-containing influent was fed to the MBBR for complete nitrification, providing nitrate for the S^{0}DA process in the UASB. In the MBBR, 99.4 % of NH_4^+ was converted to NO_3^-, yielding 49.0 ± 1.8 mg N/L of nitrate in the effluent (Fig. 4a). The effluent nitrite concentration in the MBBR in Phase II was below the detection limit. Only 0.3 mg N/L of nitrogen was lost in the nitrification reactor, with 0.10 mg N/L emitted as N_2O (Section 3.2.2), while the remaining 0.2 mg N/L was likely utilized for biomass growth.

The nitrified effluent and bypassed synthetic wastewater were mixed in a 1:1 ratio, resulting in a mixture containing 22.6 ± 1.2 mg N/L NH_4^+ and 24.7 ± 1.2 mg N/L NO_3^-, which was fed into the S^{0}DA reactor (Fig. 4b). The ammonium and nitrate removal efficiencies were 85.6 ± 8.6 % and 92.8 ± 6.3 %, respectively. The nitrite concentration in the S^{0}DA reactor consistently remained at a low level of 0.3 ± 0.5 mg N/L. The S^{0}DA reactor achieved an impressive TN removal efficiency of 89.0 ± 5.7 %, with a high NRR of 0.53 ± 0.04 kg N/(m^3·d) in Phase II. Overall, the TN removal efficiency of the NS^{0}DA ranged from 78.2 % to 100.0 % during Phase II, with an average value of 89.1 ± 5.7 % (Fig. 4c). The effluent TN of the NS^{0}DA process was as low as 5.4 ± 2.8 mg N/L.

The excellent nitrogen removal of the NS^{0}DA process stemmed from the stable and efficient performance of the S^{0}DA reactor (Fig. 4e). The ratio of removed nitrate to removed ammonium was 1.24 in the S^{0}DA reactor, closely aligning with the theoretical value of 1.06 for the S^{0}DA process. Notably, throughout the 198-d operation of the S^{0}DA reactor in Phase II, the anammox process consistently accounted for 87.3 ± 7.0 % of the nitrogen removal (Fig. S3), higher than that in Phase IC (83.6 ± 7.6 %). This result indicated that nitrate from the nitrification reactor was a reliable substrate for the subsequent S^{0}DA process. Although oxygen in the nitrifying effluent may have entered the S^{0}DA reactor, it did not adversely influence the anammox activity.

The stable performance of the S^{0}DA reactor depended on maintaining the optimal influent composition, which was a mixture of nitrification effluent and synthetic wastewater. The ratio of nitrate to ammonium was constantly maintained at 1.09, which was ideal for the S^{0}DA process. The high nitrifying activity was attributable to constant nitrate production, which enabled consistent control of the nitrate-to-ammonium ratio in the influent of S^{0}DA. Therefore, controlling this ratio is a crucial strategy for the long-term operation of the NS^{0}DA process. Suppression of NOB is a bottleneck for the application of mainstream PNA (Du et al., 2019), while the operation of NS^{0}DA is more controllable and easier to sustain in long-term operation.

The NS^{0}DA process without recirculation has distinct advantages over recirculating PDA systems. NS^{0}DA eliminates the energy consumption associated with pumping recirculated wastewater, which typically accounts for 1.5–3.5 % of the total energy consumed in

wastewater treatment (Longo et al., 2016). Additionally, the NS^{0}DA system has a higher nitrogen removal efficiency than the PDA with circulation flow. Recirculating PDA systems typically use a circulation ratio of 200–300 % (Jiang et al., 2023), resulting in a maximum nitrogen removal efficiency of only 79.5–85.4 %. In contrast, the maximum nitrogen removal efficiency for NS^{0}DA can reach 100 %. In this study, a TN removal efficiency of 89.0 ± 5.7 % was achieved, exceeding the threshold of recirculating PDA systems. In addition, optimizing the mixed ratio of nitrification effluent to raw wastewater can further improve the nitrogen removal efficiency of the NS^{0}DA process. These findings highlight the effectiveness and energy-saving benefits of the NS^{0}DA process in mainstream nitrogen removal.

3.2.2. N_2O emissions from the NS^{0}DA process

N_2O, a potent greenhouse gas, is a significant concern owing to its role in global warming, and wastewater treatment systems are a key source of N_2O emissions (Terada et al., 2017). The N_2O emission from the NS^{0}DA process was measured during the stable operation period of Phase II (Fig. 5a). In the NS^{0}DA process, 89.8 % of N_2O was emitted from the nitrification reactor (Fig. 5b). The N_2O emission factor from the nitrification reactor varied in the range of 0.05–0.39 %, with an average value of 0.21 %. By contrast, the S^{0}DA reactor accounted for only 0.02 % of the N_2O emission factor, contributing 10.2 % of the total N_2O emissions from the NS^{0}DA process.

The N_2O emission factors from mainstream anammox-based nitrogen removal processes have been noted to be 1.25 % for a pilot-scale PNA process (Hausherr et al., 2022), 5.1–6.6 % for a full-scale PNA process (Desloover et al., 2011), and 2.22 % for a lab-scale nitrification-PDA process (Zhou et al., 2020). In comparison, the NS^{0}DA process strongly represses N_2O emissions, attributable to the following factors. 1) Nitrite was not accumulated in nitrification. The nitrifying reactor in the NS^{0}DA process produced nitrate instead of nitrite, preventing nitrite accumulation. Nitrite accumulation is known to significantly increase N_2O production through nitrifier denitrification ($NH_4^+ + NO_2^- \rightarrow N_2O$), especially under oxygen-limitation conditions (Terada et al., 2017). In this study, the high DO level (> 5.0 mg/L) and undetectable nitrite concentrations prevented nitrifier denitrification. Consequently, the N_2O emission factor of the nitrification reactor was lower than those reported for partial nitrification systems (0.57–9.6 %) (Ahn et al., 2011; Hausherr et al., 2022). 2) N_2O did not function as an essential intermediate in the S^{0}DA nitrogen removal pathway. In the S^{0}DA reactor, anammox contributed to 87.3 ± 7.0 % of nitrogen removal. In contrast, denitrification was responsible for only 12.7 ± 7.0 % of nitrogen removal, where N_2O was potentially produced. Moreover, the NO_2^- concentration considerably affects N_2O emissions in denitrification. When the NO_2^- concentration was below 2 mg/L, the N_2O production was limited owing to the alleviation of nitrite inhibition on N_2O reductase (Pocquet et al., 2016; von Schulthess et al., 1994). The nitrite concentration was as low as 0.3 ± 0.5 mg N/L in the S^{0}DA reactor, and thus most of the produced N_2O was immediately reduced to nitrogen gas without accumulation.

3.3. Mechanisms for effective nitrogen removal in the S^{0}DA reactor

3.3.1. Isotope analysis to clarify the cooperation between anammox and denitrification

Isotope tracing was performed to investigate the nitrogen removal pathway and evaluate the cooperation between anammox and denitrification in the S^{0}DA reactor. Batch tests (Fig. 6a) revealed that anammox contributed 60.1–75.3 % to nitrogen removal, aligning with the value of 65.8 ± 4.1 % calculated by the nitrogen mass balance (Fig. 6b). These contributions were lower than those in the continuously operated reactor (87.3 % ± 7.0 %). This observed discrepancy likely resulted from changes in operational parameters, such as variations in sludge concentration and the ratio of elemental sulfur to nitrate (Li et al., 2022).

During the batch test, a decline in anammox's contribution to nitrogen removal was observed (Fig. 6a), consistent with the increased ratio of ΔSO_4^{2-}-S/ΔNO_3^--N (Fig. 6c). To clarify the underlying mechanism, the kinetics of nitrogen and sulfur were analyzed. Based on the trends of nitrogen and sulfate concentrations, the batch test was divided into two stages: I (0–3 h) and II (3–9 h). As shown in Fig. 6d, the specific activity of denitrification for nitrate reduction ($r_{D-NO_3^-}$) decreased from 1.50 ± 0.04 mg N/(g VSS·h) in Stage I to 1.21 ± 0.06 mg N/(g VSS·h) in Stage II. In contrast, the specific activity of denitrification for nitrite reduction ($r_{D-NO_2^-}$) increased from 0.40 ± 0.18 mg N/(g VSS·h) in Stage I to 0.67 ± 0.10 mg N/(g VSS·h) in Stage II. These results indicated a weakening of nitrate reductase's competitive advantage for electrons. Furthermore, the specific activity of anammox for nitrite reduction ($r_{A-NO_2^-}$) decreased from 1.10 ± 0.15 mg N/(g VSS·h) in Stage I to 0.54 ± 0.04 mg N/(g VSS·h) in Stage II. Overall, the increase in $r_{D-NO_2^-}$ led to a decline in anammox's contribution to nitrogen removal. Some possible explanations for the increase in $r_{D-NO_2^-}$ are as follows. The decrease in pH from 8.06 to 7.48 during the batch test alleviated the suppression of nitrite reduction (Fig. S4). Nitrite reductase obtains protons from the extracellular side of the cytoplasmic membrane, while nitrate reductase acquires the necessary protons from the interior of the cytoplasmic membrane (Cui et al., 2019a). In high pH conditions, a deficiency of protons in the periplasmic space limits nitrite reduction, causing nitrite accumulation and the diversion of more electrons towards nitrate reduction, which enhances the rate of nitrate reduction (Glass and Silverstein, 1998). Moreover, variations in electron transfer pathways, sulfur conversion mechanisms, and interactions among SOB and anammox bacteria likely influenced nitrite reduction rates and require

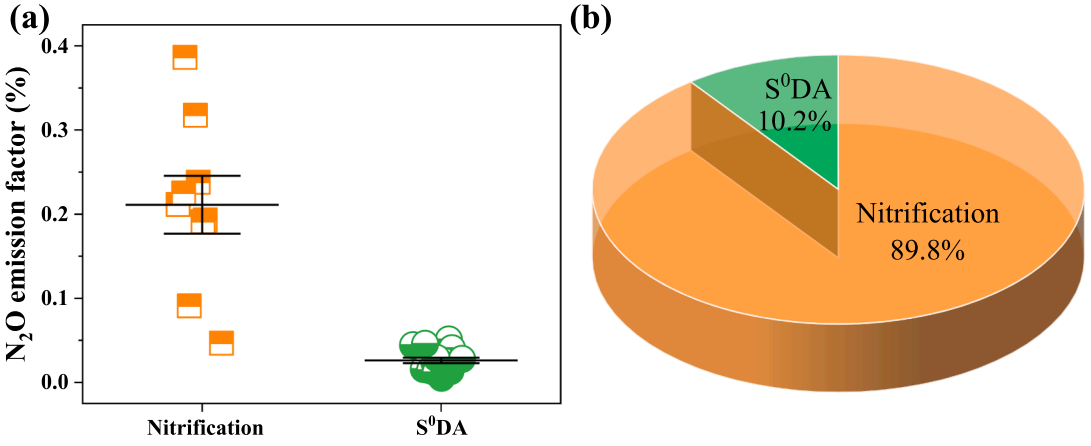

Fig. 5. N_2O emissions in the NS^{0}DA process: N_2O emission factors in nitrification and S^{0}DA reactors (a); and distribution of N_2O emissions in the NS^{0}DA process (b).

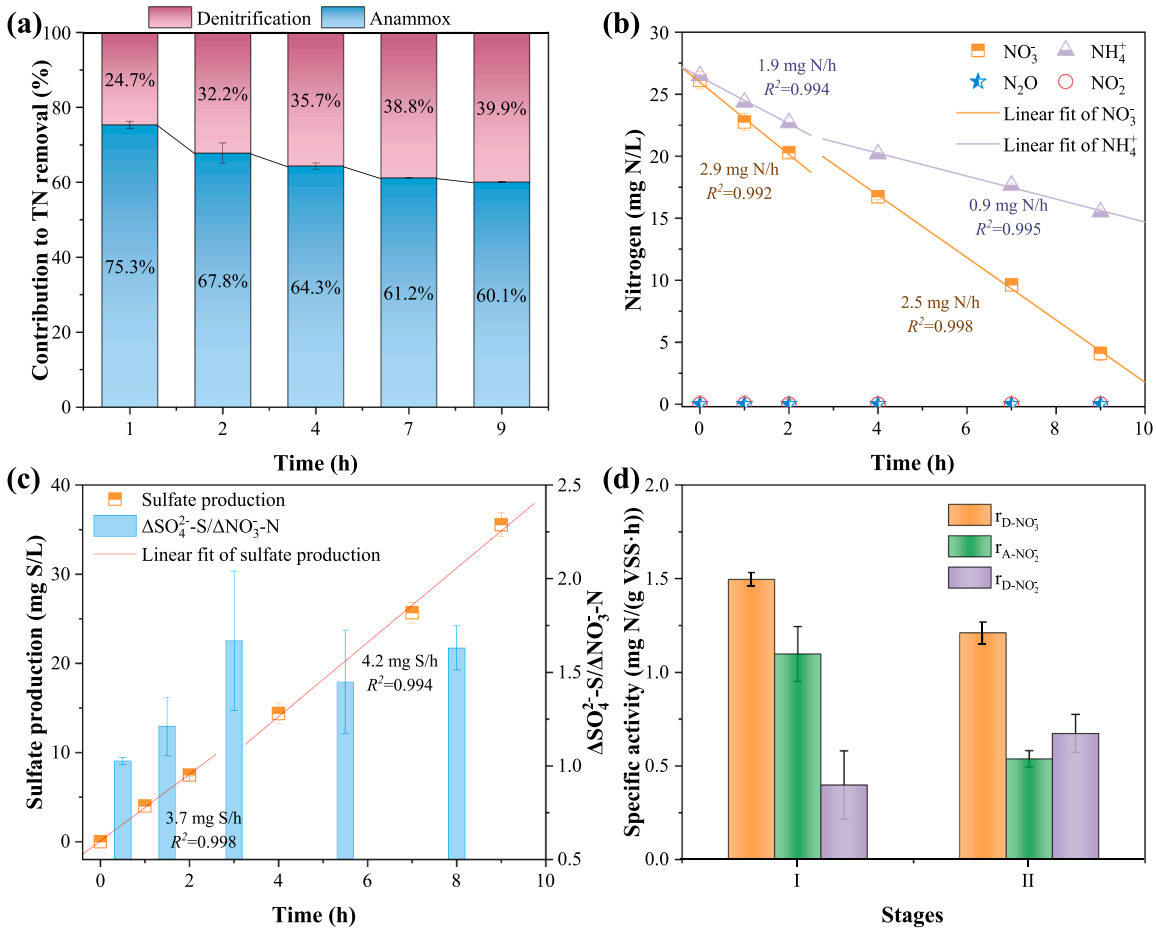

Fig. 6. Nitrogen removal pathways identified based on the $^{29}N_2/^{30}N_2$ percentage (a); variations in nitrogen (b) and sulfate (c) concentrations in the liquid phase; and specific activity of denitrification for nitrate/nitrite reduction ($r_{D-NO_3^-}/r_{D-NO_2^-}$) and specific activity of anammox for nitrite reduction ($r_{A-NO_2^-}$) (d) during the isotope batch test.

further exploration.

3.3.2. *Role of polysulfides in high-rate nitrogen removal*

In the S^0DA reactor, effective utilization of elemental sulfur by sulfur-based denitratation is a prerequisite for high-rate nitrogen removal. Sulfur-based denitratation first reduces nitrate to nitrite, followed by the reduction of nitrite to nitrogen gas by anammox. However, elemental sulfur is a limiting substrate for SOB owing to its extremely low solubility. Sulfur disproportionation results in the formation of polysulfides as an intermediate in the elemental sulfur-based denitrification system, which accelerates the elemental sulfur utilization rate (Qiu et al., 2022). SOB rapidly consumes generated polysulfides and sulfide in the presence of oxidized nitrogen (i.e., NO_3^- and NO_2^-), resulting in an undetectable level of sulfide/polysulfides (Sun et al., 2023). To confirm the occurrence of sulfur disproportionation and presence of polysulfides in the S^0DA reactor, batch tests were conducted with 1 g/L of elemental sulfur powder without oxidized nitrogen. As shown in Fig. 7a, the produced sulfide and sulfate at the end of the batch

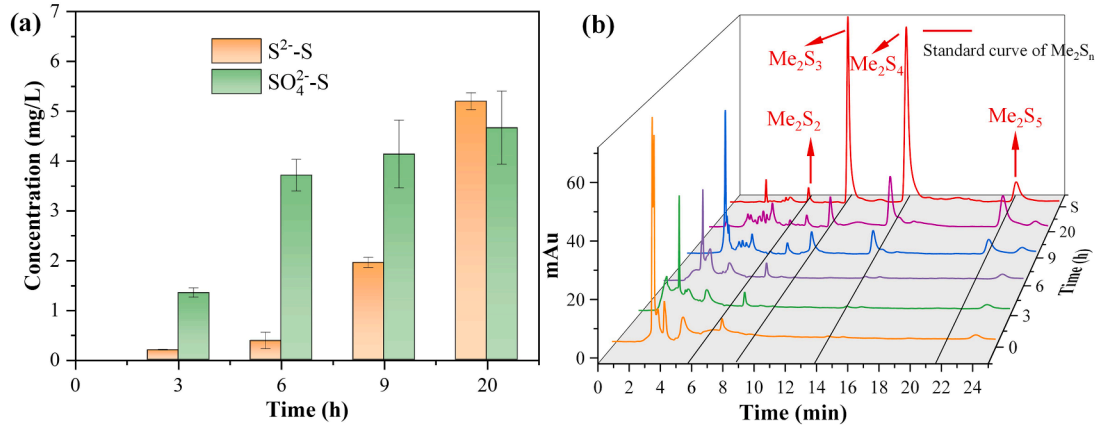

Fig. 7. Identification of different sulfur forms in the batch test: variation in sulfide/sulfate concentrations (a); and HPLC chromatogram of polysulfides (b).

test increased to 5.2 and 4.7 mg S/L, respectively. The S^{2-}-S/SO_4^{2-}-S ratio was 1.1, lower than the theoretical value (3.0) for sulfur disproportionation. The low S^{2-}-S/SO_4^{2-}-S ratio may be attributable to the formation of metal sulfides in the sludge (Fig. S5). The sulfide produced through sulfur disproportionation serves as a precursor for polysulfides formation. The formation of polysulfides in this batch test was verified through derivatization methods. As shown in Fig. 7b, the polysulfides concentration gradually increased with the formation of sulfide, and S_2^{2-}, S_3^{2-}, S_4^{2-}, and S_5^{2-} were detected during the batch test. These results indicate that sulfide can potentially be produced by sulfur disproportionation in the anaerobic zone, and the elemental sulfur is therefore activated by polysulfides formation. Thus, the self-acceleration of sulfur utilization driven by polysulfides supports high-rate nitrogen removal in the S^0DA reactor. The polysulfides formation appears to be a breakthrough in addressing the slow denitrification rate of elemental sulfur-based nitrogen removal.

3.4. Microbial analysis

Changes in the microbial community in the NS^{0}DA system during the experiment were explored through 16S rRNA gene sequencing and metagenomics. In the nitrification reactor, *Nitrosomonas* (ammonia-oxidizing bacteria) and *Nitrospira* (NOB) were the dominant functional genera (Chen et al., 2020), as shown in Fig. 8a. The relative abundances of *Nitrosomonas* and *Nitrospira* throughout the operation were 14.88–16.38 % and 8.16–16.16 %, respectively. The enrichment of nitrifying bacteria guaranteed stable complete nitrification in the MBBR.

As shown in Figs. 8b and S6, both 16S rRNA gene sequencing and fluorescence in situ hybridization (FISH) analyses confirmed the coexistence of AnAOB and SOB in the S^0DA reactor. In the S^0DA reactor, the dominant AnAOB were *Candidatus* Brocadia and *Candidatus* Kuenenia. The relative abundance of *Candidatus* Brocadia increased from 0.69 % to 1.09 % with the increase in NLR from Phase IA to Phase IB. However, it decreased to 0.28 % when the temperature dropped from 30 °C (Phase

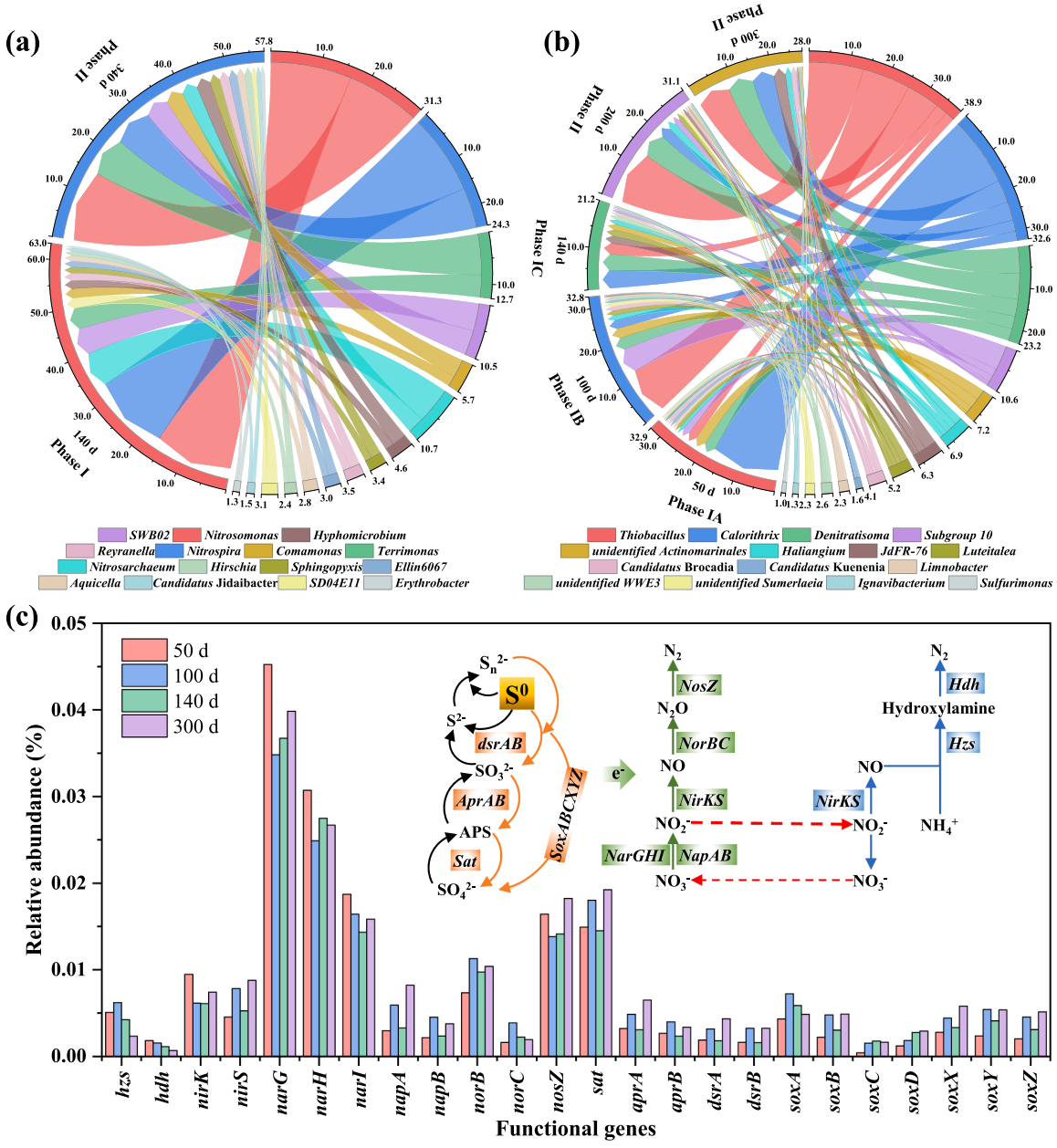

Fig. 8. Microbial communities at the genus level in the nitrification (a) and S^0DA reactors (b); and functional genes involved in sulfur and nitrogen metabolisms in the S^0DA reactor (c).

IB) to 25 °C (Phase IC) and then gradually increased to 1.30 % by the end of the experiment. The relative abundance of *Candidatus* Kuenenia gradually decreased from 0.77 % on day 50 to 0.03 % on day 260. The low relative abundance of AnAOB was likely attributable to the limitations of 16S rRNA gene sequencing, as the FISH results showed high abundance in the S^0DA reactor (Fig. S6). *Candidatus* Kuenenia exhibits a lower nitrite affinity compared with *Candidatus* Brocadia (Lotti et al., 2014) and thus dominates AnAOB groups under nitrite-limited conditions, as observed in certain PDA systems treating high-strength wastewater containing nitrate and ammonium (Deng et al., 2021; Li et al., 2019). However, in this study, *Candidatus* Brocadia was the dominant AnAOB in the S^0DA reactor despite the low nitrite concentration (0.3 ± 0.5 mg N/L) in the system. Certain species of *Candidatus* Brocadia, such as *Candidatus* Brocadia sp.40 and *Candidatus* Brocadia sinica, exhibited higher specific growth rates compared with *Candidatus* Kuenenia, enabling their dominance under low-nitrogen conditions (Zhang and Okabe, 2020). In addition to the influent nitrogen concentration, other factors such as temperature and polysulfide may have influenced anammox community composition.

The relative abundance of *Thiobacillus*, the dominant SOB in the S^0DA reactor, increased from 2.32 % in Phase IA to 11.97 % in Phase IB, decreased to 2.87 % in Phase IC, and finally recovered to 8.32 % by the end of Phase II. The subdominant SOB was *Sulfurimonas*, which maintained a relative abundance of 0.06–0.41 % throughout the experiment. *Thiobacillus* and *Sulfurimonas* are widely recognized for their roles in sulfur (e.g., sulfide, elemental sulfur, and thiosulfate)-based partial denitrification combined with anammox (Deng et al., 2021; Wang et al., 2023b), where they supply nitrite for anammox. However, these SOBs typically exhibit a low uptake rate of elemental sulfur, especially for the pure cultured strains, owing to the challenging bioaccessibility of elemental sulfur (Di Capua et al., 2016). Notably, some sulfate-reducing bacteria (SRB), such as *Sva0081*_sediment_group, *Desulfoprunum, Desulfomonile*, and *Desulforhabdus*, which are capable of reducing sulfur/sulfate to sulfide, were identified in the S^0DA reactor (Fig. S7). Among these, *Desulfomonile* is capable of the dismutation of sulfur compounds (Slobodkin and Slobodkina, 2019), which may account for the sulfide production observed in the batch test. Moreover, the presence of SRBs provides further evidence for sulfide production in the S^0DA reactor. The produced sulfide may undergo nucleophilic reaction with elemental sulfur to produce polysulfides, thereby enhancing nitrogen removal in the S^0DA reactor.

To further investigate the interaction between sulfur and nitrogen metabolisms in the S^0DA reactor, the functional genes encoding sulfur and nitrogen metabolic enzymes were analyzed by metagenomics, and the results are shown in Fig. 8c. Microbes mainly access elemental sulfur through direct transport and indirect transport involving polysulfides (Zhang et al., 2021). The genes encoding the dissimilatory sulfate reduction pathway (e.g., *sat, aprAB* and *dsrAB*) were detected, verifying the potential for polysulfides production. After entering the cell, elemental sulfur/polysulfides are converted into sulfate primarily through the sulfur-oxidizing enzyme (Sox)-dependent pathway and the Sox-independent pathway (Cui et al., 2019b), which was supported by the identification of genes linked to the Sox-dependent pathway (*soxABCDXYZ*) and the Sox-independent pathway (*dsrAB, aprAB* and *sat*). The nitrogen metabolism in the S^0DA system was also evaluated in the S^0DA system. Notably, the relative abundance of *napAB* (0.005 %−0.012 %) and *narGHI* (0.076 %−0.095 %) encoding nitrate reductase was higher than that of *nirKS* (0.014 %−0.016 %) encoding nitrite reductase. This finding indicates a significant potential for nitrite accumulation in denitrification, guaranteeing a sufficient supply of nitrite for anammox. Subsequently, the nitrite produced by SOB and ammonium in the wastewater were eliminated by AnAOB via a series of enzymes, including nitrite reductase encoded by *nirKS*, hydrazine synthase subunit encoded by *hzs* (0.002 %−0.006 %), and hydrazine dehydrogenase encoded by *hdh* (0.001 %−0.002 %). The symbiotic relationship between SOB and AnAOB was further validated through genetic evidence of synergistic nitrogen and sulfur metabolic pathways, which explained the excellent nitrogen removal performance in the NS^0DA process.

3.5. Implications

This study demonstrates that NS^0DA is a reliable and cost-efficient technology for mainstream nitrogen removal. NS^0DA can reduce oxygen consumption by 50 % compared with the traditional nitrogen removal process. Although this value is slightly lower than that of the PNA process (60 %), NS^0DA eliminates the need for complex control systems for NOB suppression. The electron donor cost (elemental sulfur) is only 0.05 USD/kg N in the NS^0DA system, representing a reduction of 75.4–92.1 % relative to the organics-based PDA process (Table S3) (Di Capua et al., 2019). Moreover, the NS^0DA process reduces sulfate production by 67.5 % compared with elemental sulfur-based denitrification. The average sulfate concentration in the effluent of NS^0DA is 46.8 mg S/L (equal to 140.4 mg SO_4^{2-}/L), which is well below drinking water standards (250 mg SO_4^{2-}/L) (WHO, 2004). Hence, the NS^0DA process offers a safe, cost-effective, and efficient solution for mainstream nitrogen removal.

To ensure sustainable wastewater treatment, it is preferable to capture organics for energy recovery rather than oxidizing them to carbon dioxide. Several physicochemical and biological processes can be applied for harvesting organics from wastewater, such as high-rate activated sludge, chemically enhanced primary treatment, and anaerobic membrane bioreactors (Guven et al., 2022). However, effectively removing nitrogen from carbon-capturing effluent remains a significant bottleneck to achieving sustainable wastewater treatment. The NS^0DA process, as a fully autotrophic nitrogen removal system, can be integrated with these carbon-capturing units to realize energy/carbon neutrality in mainstream wastewater treatments. This integration demonstrates significant potential for practical engineering applications. However, this integrated process still involves various challenges that necessitate further exploration, including the mechanism of elemental sulfur bio-oxidation, microscale distributions of SOB and AnAOB, and the applicability of NS^0DA in real municipal wastewater.

5. Conclusion

This study developed a novel NS^0DA process for nitrogen removal, consisting of a nitrification reactor and an S^0DA reactor. The long-term performance of the NS^0DA process in mainstream conditions was investigated. The following conclusions were derived.

- The NS^0DA system demonstrated an outstanding TN removal efficiency (89.1 ± 5.7 %) for treating mainstream wastewater at 25 °C. The S^0DA reactor operated with an HRT of 2 h, and its NRR was stably maintained at 0.53 kg N/(m^3·d).
- Anammox and denitrification were responsible for 87.3 % and 12.7 % of the TN removal, respectively. Moreover, isotope analysis verified the high activity of anammox in the NS^0DA system.
- The absence of nitrite formation in the nitrification reactor and high anammox activity in the S^0DA resulted in a low N_2O emission (0.23 %) factor from the NS^0DA system.
- The formation of polysulfides improved the bioavailability of the elemental sulfur and supported the high NRR in the NS^0DA process.
- The functional bacteria in the nitrification reactor were *Nitrosomonas* and *Nitrospira*. Additionally, the coexistence of AnAOB (*Candidatus* Brocadia), SOB (*Thiobacillus*), and several SRBs in the S^0DA reactor was confirmed.

CRediT authorship contribution statement

Yuanjun Liu: Writing – original draft, Methodology, Investigation. **Yangfan Deng:** Writing – review & editing, Supervision, Funding acquisition, Conceptualization. **Mark C.M. van Loosdrecht:** Writing –

review & editing. **Guanghao Chen:** Writing – review & editing, Supervision, Resources, Funding acquisition.

Declaration of competing interest

The authors declare that they have no known competing financial interests or personal relationships that could have appeared to influence the work reported in this paper.

Acknowledgement

This study was supported by the National Natural Science Foundation of China (52200071), the Hong Kong Research Grants Council (T21-604/19-R), and the Hong Kong Innovation and Technology Commission (ITC-CNERC14EG03).

Supplementary materials

Supplementary material associated with this article can be found, in the online version, at doi:10.1016/j.watres.2025.123836.

Data availability

Data will be made available on request.

References

Ahn, J., Kwan, T., Chandran, K., 2011. Comparison of partial and full nitrification processes applied for treating high-strength nitrogen wastewaters: microbial ecology through nitrous oxide production. Environ. Sci. Technol. 45, 2734–2740.
Almeida, J., Reis, M., Carrondo, M., 1995. Competition between nitrate and nitrite reduction in denitrification by *Pseudomonas fluorescens*. Biotechnol. Bioeng. 46, 476–484.
Beffa, T., Berczy, M., Aragno, M., 1991. Chemolithoautotrophic growth on elemental sulfur (S^0) and respiratory oxidation of S^0 by *thiobacillus versutus* and another sulfur-oxidizing bacterium. FEMS Microbiol. Lett. 84, 285–290.
Boulegue, J., 1978. Solubility of elemental sulfur in water at 298-K. Phosphorus Sulfur Silicon Related Elements 5, 127–128.
Cao, Y., van Loosdrecht, M.C., Daigger, G.T., 2017. Mainstream partial nitritation-anammox in municipal wastewater treatment: status, bottlenecks, and further studies. Appl. Microbiol. Biot. 101, 1365–1383.
Chen, F., Li, X., Gu, C., Huang, Y., Yuan, Y., 2018. Selectivity control of nitrite and nitrate with the reaction of S^0 and achieved nitrite accumulation in the sulfur autotrophic denitrification process. Bioresour. Technol. 266, 211–219.
Chen, G.H., van Loosdrecht, M.C., Ekama, G.A., Brdjanovic, D., 2020. Biological Wastewater treatment: principles, Modeling and Design. IWA publishing, London.
Cui, Y.X., Biswal, B.K., Guo, G., Deng, Y.F., Huang, H., Chen, G.H., Wu, D., 2019a. Biological nitrogen removal from wastewater using sulphur-driven autotrophic denitrification. Appl. Microbiol. Biot. 103, 6023–6039.
Cui, Y.X., Biswal, B.K., van Loosdrecht, M.C.M., Chen, G.H., Wu, D., 2019b. Long term performance and dynamics of microbial biofilm communities performing sulfur-oxidizing autotrophic denitrification in a moving-bed biofilm reactor. Water. Res. 166, 115038.
Deng, Y., Wu, D., Huang, H., Cui, Y., van Loosdrecht, M.C., Chen, G., 2021. Exploration and verification of the feasibility of sulfide-driven partial denitrification coupled with anammox for wastewater treatment. Water. Res. 193, 116905.
Deng, Y., Zan, F., Huang, H., Wu, D., Tang, W., Chen, G., 2022. Coupling sulfur-based denitrification with anammox for effective and stable nitrogen removal: a review. Water. Res. 224, 119051.
Desloover, J., De Clippeleir, H., Boeckx, P., Du Laing, G., Colsen, J., Verstraete, W., Vlaeminck, S.E., 2011. Floc-based sequential partial nitritation and anammox at full scale with contrasting N_2O emissions. Water. Res. 45, 2811–2821.
Di Capua, F., Ahoranta, S., Papirio, S., Lens, P., Esposito, G., 2016. Impacts of sulfur source and temperature on sulfur-driven denitrification by pure and mixed cultures of *thiobacillus*. Process. Biochem. 51, 1576–1584.
Di Capua, F., Pirozzi, F., Lens, P., Esposito, G., 2019. Electron donors for autotrophic denitrification. Chem. Eng. J. 362, 922–937.
Du, R., Peng, Y., Ji, J., Shi, L., Gao, R., Li, X., 2019. Partial denitrification providing nitrite: opportunities of extending application for anammox. Environ. Int. 131, 105001.
Glass, C., Silverstein, J., 1998. Denitrification kinetics of high nitrate concentration water: pH effect on inhibition and nitrite accumulation. Water. Res. 32, 831–839.
Guven, H., Ersahin, M.E., Ozgun, H., 2022. Chapter 7 - energy self-sufficiency in wastewater treatment plants: perspectives, challenges, and opportunities. Clean Energy Resource Recovery 105–122.
Hausherr, D., Niederdorfer, R., Burgmann, H., Lehmann, M., Magyar, P., Mohn, J., Morgenroth, E., Joss, A., 2022. Successful year-round mainstream partial nitritation anammox: assessment of effluent quality, performance and N_2O emissions. Water. Res. X. 16, 100145.
Jiang, C., Deng, Y., Zou, X., Siriweera, B., Wu, D., Chen, G., 2023. Sulphate reduction, mixed sulphide- and thiosulphate-driven autotrophic denitrification, NItrification, and anammox (SANIA) integrated process for sustainable wastewater treatment. Water. Res. 247, 120824.
Kamyshny Jr., A., Goifman, A., Gun, J., Rizkov, D., Lev, O., 2004. Equilibrium distribution of polysulfide ions in aqueous solutions at 25°C: a new approach for the study of polysulfides' equilibria. Environ. Sci. Technol. 38, 6633–6644.
Kanehisa, M., Furumichi, M., Tanabe, M., Sato, Y., Morishima, K., 2017. KEGG: new perspectives on genomes, pathways, diseases and drugs. Nucleic. Acids. Res. 45, D353–D361.
Kartal, B., Kuenen, J.G., van Loosdrecht, M.C., 2010. Sewage treatment with anammox. Science (1979) 328, 702–703.
Koenig, A., Liu, L., 2004. Autotrophic denitrification of high-salinity wastewater using elemental sulfur: batch tests. Water. Environ. Res. 76, 37–46.
Kumar, M., Lin, J.G., 2010. Co-existence of anammox and denitrification for simultaneous nitrogen and carbon removal–strategies and issues. J. Hazard. Mater. 178, 1–9.
Le, T., Peng, B., Su, C., Massoudieh, A., Torrents, A., Al-Omari, A., Murthy, S., Wett, B., Chandran, K., DeBarbadillo, C., Bott, C., De Clippeleir, H., 2019. Impact of carbon source and COD/N on the concurrent operation of partial denitrification and anammox. Water. Environ. Res. 91, 185–197.
Li, W.W., Yu, H.Q., Rittmann, B.E., 2015. Reuse water pollutants. Nature 528, 29–31.
Li, X., Shi, M., Zhang, M., Li, W., Xu, P.L., Wang, Y.Y., Yuan, Y., Huang, Y., 2022. Progresses and challenges in sulfur autotrophic denitrification-enhanced anammox for low carbon and efficient nitrogen removal. Crit. Rev. Env. Sci. Tec. 52, 4379–4394.
Li, X., Yuan, Y., Huang, Y., Bi, Z., 2019. Simultaneous removal of ammonia and nitrate by coupled S^0-driven autotrophic denitrification and anammox process in fluorine-containing semiconductor wastewater. Sci. Total. Environ. 661, 235–242.
Li, Y., Chen, B., Zhang, X., Luo, Z., Lei, M., Song, T., Long, Z., Li, J., Ma, J., 2023. Elemental sulfur autotrophic partial denitrification (S^0-PDN) with high pH and free ammonia control strategy for low-carbon wastewater: from performance to microbial mechanism. Chem. Eng. J. 474.
Longo, S., d'Antoni, B.M., Bongards, M., Chaparro, A., Cronrath, A., Fatone, F., Lema, J. M., Mauricio-Iglesias, M., Soares, A., Hospido, A., 2016. Monitoring and diagnosis of energy consumption in wastewater treatment plants. A state of the art and proposals for improvement. Appl. Energ. 179, 1251–1268.
Lotti, T., Kleerebezem, R., Hu, Z., Kartal, B., de Kreuk, M.K., van Erp Taalman Kip, C., Kruit, J., Hendrickx, T.L., van Loosdrecht, M.C, 2015. Pilot-scale evaluation of anammox-based mainstream nitrogen removal from municipal wastewater. Environ. Technol. 36, 1167–1177.
Lotti, T., Kleerebezem, R., Lubello, C., van Loosdrecht, M.C.M., 2014. Physiological and kinetic characterization of a suspended cell anammox culture. Water. Res. 60, 1–14.
McCarty, P.L., 2018. What is the best biological process for nitrogen removal: when and why? Environ. Sci. Technol. 52, 3835–3841.
McCarty, P.L., Bae, J., Kim, J., 2011. Domestic wastewater treatment as a net energy producer–can this be achieved? Environ. Sci. Technol. 45, 7100–7106.
Mulder, A. 1992. Anoxic ammonia oxidation. US Patent 5078884.
Niederdorfer, R., Hausherr, D., Palomo, A., Wei, J., Magyar, P., Smets, B.F., Joss, A., Burgmann, H., 2021. Temperature modulates stress response in mainstream anammox reactors. Commun. Biol. 4, 23.
Nielsen, H.B., Almeida, M., Juncker, A.S., Rasmussen, S., Li, J., Sunagawa, S., Plichta, D. R., Gautier, L., Pedersen, A.G., Le Chatelier, E., Pelletier, E., Bonde, I., Nielsen, T., Manichanh, C., Arumugam, M., Batto, J.M., Quintanilha Dos Santos, M.B., Blom, N., Borruel, N., Burgdorf, K.S., Boumezbeur, F., Casellas, F., Dore, J., Dworzynski, P., Guarner, F., Hansen, T., Hildebrand, F., Kaas, R.S., Kennedy, S., Kristiansen, K., Kultima, J.R., Leonard, P., Levenez, F., Lund, O., Moumen, B., Le Paslier, D., Pons, N., Pedersen, O., Prifti, E., Qin, J., Raes, J., Sorensen, S., Tap, J., Tims, S., Ussery, D.W., Yamada, T., Meta, H.I.T.C., Renault, P., Sicheritz-Ponten, T., Bork, P., Wang, J., Brunak, S., Ehrlich, S.D., Meta, H.I.T.C., 2014. Identification and assembly of genomes and genetic elements in complex metagenomic samples without using reference genomes. Nat. Biotechnol. 32, 822–828.
Pocquet, M., Wu, Z., Queinnec, I., Sperandio, M., 2016. A two pathway model for N_2O emissions by ammonium oxidizing bacteria supported by the NO/N_2O variation. Water. Res. 88, 948–959.
Qiu, Y., Gong, X., Zhang, L., Zhou, S., Li, G., Jiang, F., 2022. Achieving a novel polysulfide-involved sulfur-based autotrophic denitrification process for high-rate nitrogen removal in elemental sulfur-packed bed reactors. ACS EST Eng. 2, 1504–1513.
Rice, E.W., Baird, R.B., Eaton, A.D., Clesceri, L.S., 2005. Standard Methods for the Examination of Water and Wastewater, 22 ed. American Public Health Association, Washington, D.C.
Sierra-Alvarez, R., Beristain-Cardoso, R., Salazar, M., Gomez, J., Razo-Flores, E., Field, J. A., 2007. Chemolithotrophic denitrification with elemental sulfur for groundwater treatment. Water. Res. 41, 1253–1262.
Slobodkin, A.I., Slobodkina, G.B., 2019. Diversity of sulfur-disproportionating microorganisms. Microbiology (N. Y) 88, 509–522.
Strous, M., Heijnen, J., Kuenen, J.G., Jetten, M., 1998. The sequencing batch reactor as a powerful tool for the study of slowly growing anaerobic ammonium-oxidizing microorganisms. Appl. Microbiol. Biot. 50, 589–596.
Sun, Y., Zhai, S., Qian, Z., Yi, S., Zhuang, W., Cheng, H., Zhang, X., Wang, A., 2023. Managing microbial sulfur disproportionation for optimal sulfur autotrophic denitrification in a pilot-scale elemental sulfur packed-bed bioreactor. Water. Res. 243, 120356.

Takekawa, M., Park, G., Soda, S., Ike, M., 2014. Simultaneous anammox and denitrification (SAD) process in sequencing batch reactors. Bioresour. Technol. 174, 159–166.
Terada, A., Sugawara, S., Hojo, K., Takeuchi, Y., Riya, S., Harper Jr., W.F., Yamamoto, T., Kuroiwa, M., Isobe, K., Katsuyama, C., Suwa, Y., Koba, K., Hosomi, M., 2017. Hybrid nitrous oxide production from a partial nitrifying bioreactor: hydroxylamine interactions with nitrite. Environ. Sci. Technol. 51, 2748–2756.
Thamdrup, B., Dalsgaard, T., 2002. Production of N_2 through anaerobic ammonium oxidation coupled to nitrate reduction in marine sediments. Appl. Environ. Microbiol. 68, 1312–1318.
von Schulthess, R., Wild, D., Gujer, W., 1994. Nitric and nitrous oxides from denitrifying activated sludge at low oxygen concentration. Water Sci. Tech. 30, 123–132.
Wang, K., Li, J., Gu, X., Wang, H., Li, X., Peng, Y., Wang, Y., 2023a. How to provide nitrite robustly for anaerobic ammonium oxidation in mainstream nitrogen removal. Environ. Sci. Technol. 57, 21503–21526.
Wang, Y., Bott, C., Nerenberg, R., 2016. Sulfur-based denitrification: effect of biofilm development on denitrification fluxes. Water. Res. 100, 184–193.
Wang, Z., Gao, J., Dai, H., Yuan, Y., Zhao, Y., Li, D., Cui, Y., 2023b. Partial S^0-driven autotrophic denitrification process facilitated the quick natural enrichment of anammox bacteria at room temperature. Sci. Total. Environ. 855, 158916.
WHO, 2004. Sulfate in drinking-water: Background Document for Development of WHO Guidelines for Drinking-Water Quality. World Health Organization.
Yuan, Y., Li, X., Li, W., Shi, M., Zhang, M., Xu, P., Li, B., Huang, Y., 2022. Effects of different reduced sulfur forms as electron donors in the start-up process of short-cut sulfur autotrophic denitrification. Bioresour. Technol. 354, 127194.
Zhang, K., Kang, T., Yao, S., Liang, B., Chang, M., Wang, Y., Ma, Y., Hao, L., Zhu, T., 2020. A novel coupling process with partial nitritation-anammox and short-cut sulfur autotrophic denitrification in a single reactor for the treatment of high ammonium-containing wastewater. Water. Res. 180, 115813.
Zhang, L., Okabe, S., 2020. Ecological niche differentiation among anammox bacteria. Water. Res. 171, 115468.
Zhang, L., Qiu, Y.Y., Zhou, Y., Chen, G.H., van Loosdrecht, M.C.M., Jiang, F., 2021. Elemental sulfur as electron donor and/or acceptor: mechanisms, applications and perspectives for biological water and wastewater treatment. Water. Res. 202, 117373.
Zhou, X., Song, J., Wang, G., Yin, Z., Cao, X., Gao, J., 2020. Unravelling nitrogen removal and nitrous oxide emission from mainstream integrated nitrification-partial denitrification-anammox for low carbon/nitrogen domestic wastewater. J. Environ. Manage 270, 110872.